FIFTH AUSTRALASIAN CONFERENCE

on

HYDRAULICS AND FLUID MECHANICS

at

University of Canterbury, Christchurch, New Zealand

1974 December 9 to December 13

NUMERICAL ANALYSIS OF VERTICAL WATER MOVEMENT IN A BOUNDED PROFILE

by

K.K. Watson and A.A. Curtis

SUMMARY

The usual assumption made in soil-water studies that the effect of the air phase on the flow process is negligible is discussed in relation to certain profile configurations where such an assumption is not valid. A computer-based numerical solution of the equation describing water movement in an unsaturated soil is then modified by the inclusion of a time-dependent boundary condition thus allowing the modelling of the air compression effect during infiltration. This analysis also satisfactorily models the drainage along primary draining scanning curves which occurs in the upper part of the profile as the air pressure increases. The analysis is limited to the Darcy flow regime which, for the system considered, terminates when the excess air pressure equals the air entry value of the porous material. Detailed results are presented for a sand and a sandy loam. Profile depths of 200 cm and 1,000 cm have been analysed and detailed comparisons made of the effect of the air compression on the shape of the wetting front. The effect on cumulative infiltration is also noted.

Associate Professor and Research Fellow respectively, School of Civil Engineering, The University of New South Wales, Kensington.

INTRODUCTION

The analysis of water movement in unsaturated porous materials usually assumes that the effect of the air phase on the flow process is negligible. Such an assumption is common when analysing the infiltration of water into a soil profile. Because of the large difference between the viscosities of air and water, only a small error results when the effect on the advancing wet front of the flow of the pore air is neglected. In addition, it has also been tacitly assumed in most infiltration studies (1) that continuity exists between the air phase ahead of the wet front and the atmosphere. In many systems these are valid assumptions; however, certain profile configurations can occur which prevent the escape of the air displaced by an advancing wet front. This situation may arise when flood irrigation is practised over large areas with soils which have a shallow water table or where an impermeable substratum exists in the profile. In such cases two types of analysis are possible. The more fundamental approach considers the fluids within the soil system to be a two-phase entity and, accordingly, writes the flow equations in terms of both the water and air phases (2). This approach is essential in certain interface problems but is unnecessarily complicated for a homogeneous bounded profile. In a bounded system we are more concerned with the compression of the air phase and the inhibiting effect this has on the infiltration process than with the actual movement of the air.

Powers (3), Free and Palmer (4) and Wilson and Luthin (5) have studied the behaviour of certain bounded systems experimentally. Youngs and Peck (6) have presented a concise theoretical introduction of the interaction existing between moisture profile development and air compression during infiltration into bounded porous bodies. The present study follows this general approach and considers vertical water movement into a bounded column using a computer-based numerical solution of the one-dimensional unsaturated flow equation with appropriate adjustment at each time step of the relevant parameters as the air pressure increases. The solution presented is only applicable to the Darcy domain. This necessarily limits the numerical solution of the infiltration process to that point in time when the air pressure increase is equal to the air entry value of the porous material. Beyond this time there would be a movement of air up to the surface and the conditions for Darcy flow in an unsaturated porous material would no longer hold. Peck (7,8) has discussed the conditions existing in the soil profile before and after air begins to escape through the surface.

NUMERICAL ANALYSIS

The equation describing the vertical, one-dimensional, isothermal movement of water in a rigid, homogeneous porous material may be written

$$C(h)\,\partial h/\partial t = \partial[K(h)\,\partial h/\partial z]/\partial z + \partial K(h)/\partial z \qquad (1)$$

where

h = soil-water pressure (cm of water)

$K(h)$ = hydraulic conductivity (cm min^{-1})

z = vertical ordinate, positive upwards (cm)

$C(h)$ = specific water capacity = $d\theta/dh$

θ = volumetric water content (cm^3 cm^{-3})

By establishing appropriate finite difference approximations to equation (1) several computer-based numerical solutions have been obtained for various boundary conditions (9,10,11). In these solutions it has been assumed that the gradients of air pressure in the soil profile can be neglected. For the present study the initial condition is assumed to be that of uniform water content (θ_i) and hence uniform soil-water pressure (h_i). The initial condition to be applied to equation (1) for a profile of depth L may therefore be written

$$t = 0,\ h = h_i,\ 0 \geq z \geq -L \qquad (2)$$

Since there is no flux across the lower boundary we may write the boundary condition as

$$0 < t < t_d,\quad \partial h/\partial z = -1,\ z = -L \qquad (3)$$

where t_d is the time at which Darcy domain behaviour terminates and the air begins to escape from the profile.

It should be noted that the $h(\theta)$ relationship is strongly hysteretic whereas no measurable hysteresis has been found in the $K(\theta)$ relationship. However, the hysteresis of $h(\theta)$ is reflected in $K(h)$. In this study the soil-water pressure (h) is defined as the hydrostatic pressure of the pore water relative to the pressure of the air contained in the pore space. If H is defined as the hydraulic head at any point in the soil-water system relative to free water at atmospheric

pressure and p is the air pressure in excess of atmospheric pressure in the pore air then

$$H = h + p + z \tag{4}$$

If sufficient water is supplied to the soil surface to meet the infiltration demands of the system, yet under a negligible surface head of water, the top boundary condition during infiltration may be written

$$t > 0,\ H = 0,\ z = 0 \tag{5}$$

If at any time t less than t_d the quantity of water which has entered the profile is q then the air pressure (p) in excess of atmospheric pressure (p_a) in the enclosed air space may be calculated from Boyle's Law since isothermal conditions have been specified.

The excess air pressure may then be found from

$$p(t) = p_a \times q/[(\theta_{sat}-\theta_i)L - q] \tag{6}$$

where θ_{sat} = porosity of the porous material.

$$\text{Now}\quad q = \int_{-L}^{0} (\theta-\theta_i)dz$$

$$\therefore\ p(t) = \frac{p_a \int_{-L}^{0} (\theta-\theta_i)dz}{(\theta_{sat}-\theta_i)L - \int_{-L}^{0} (\theta-\theta_i)dz} \tag{7}$$

Since the free water at the surface is at atmospheric pressure, then H=0 at z=0 and the upper boundary condition may alternatively be written

$$t > 0,\ h = -p(t),\ z=0 \tag{8}$$

As Youngs and Peck (6) point out equation (8) indicates that the problem under consideration (the infiltration of water under negligible surface head into a bounded column) is identical with a flow system where infiltration occurs with the surface in contact with water at a pressure -p(t) and where there is no restraint to the movement of the escaping air. This time-dependent pressure transformation is particularly useful for analysing a bounded system by numerical methods. At t=0 the infiltration analysis is commenced with a surface pressure value of h=0. At each succeeding time step as infiltration proceeds the value of p is calculated and introduced as the surface boundary condition for the next time step. By this procedure the pressure transformation is made time dependent and the system can be analysed using existing numerical techniques with the incorporation of only minor modifications.

A particular advantage of the analysis given in this paper is that the hysteresis effects which become significant as the infiltration process continues are able to be readily included in the analysis. The only additional requirement is that the primary draining scanning curves must be included as part of the $h(\theta)$ data. The phenomenon involving hysteresis which develops during infiltration was described by Youngs and Peck (6) and is discussed below.

Initially the excess air pressure p is zero and the surface wets immediately to saturation. Accordingly, the surface material which is initially represented by point A (h_i,θ_i) in Figure 1 wets up along the boundary wetting curve to point B (0,θ_{sat}). As the air pressure increases and and the value of h at the surface assumes negative values the surface material will commence to 'drain' along the boundary draining curve. However, since the boundary draining curve is horizontal between B and C (the air entry value for the porous material) and, since $t = t_d$ will correspond to the time when p(t) also reaches the air entry value, the surface material will remain saturated whenever $t \leq t_d$.

As infiltration proceeds and as the excess air pressure increases the porous material at points below the surface also wets up along the boundary wetting curve from A. However, unlike 'normal' infiltration for which there is no air compression effect, many points in the profile after wetting will not wet to saturation and may even start to drain. This occurs because continuous water movement into the profile requires a decrease of the hydraulic head of the soil water down the profile.

Since the pressure of the air increases during infiltration resulting in the surface soil-water pressure becoming more negative with time, h for points below the surface must assume values that allow the downward vertical movement of water to continue. For a vertical column the implications of this in regard to the shape of the $h(\theta)$ profile at a certain time are less predictable in detail than for a horizontal column (6) since the hydraulic head has both soil water and gravity components for vertical flow. However, the same general trends occur, namely, that at any given time a pressure transition will occur at some depth (z_t) in the profile where $\partial h/\partial t = 0$. Points above z_t will either be saturated or will be draining along primary draining scanning curves (see Figure 1) and points below z_t will continue to wet up along the boundary wetting curve. As infiltration proceeds the transition point will move down the column. The computer programme is able to cope readily with this drainage condition along primary draining curves by testing every point in the profile at each iteration for pressure reversal; as soon as this occurs the appropriate $h(\theta)$ primary draining scanning curve (or an interpolated curve if necessary) is followed for the remainder of the numerical analysis rather than the boundary wetting curve which had been followed up to that time. In the results presented in the next section an example will be given of the drainage phenomenon discussed in this paragraph.

RESULTS AND DISCUSSION

The two porous materials chosen for this study were a uniform silica sand (#17 sand) and Rubicon sandy loam. The hydrologic characteristics of this latter material were obtained by Topp (12). The $h(\theta)$ and $K(\theta)$ relationships for #17 sand are given in Figs. 2 and 3 and those for the sandy loam in Figs.4 and 5. The water contents at which 'saturation' occurs are 0.292 $cm^3\ cm^{-3}$ and 0.380 $cm^3\ cm^{-3}$ respectively. It should be noted that when repeatable boundary hysteresis loops are required in an analysis the term 'saturation', as commonly used, does not necessarily infer that the entire pore space is filled with water. When a pore space is drained and refilled it is unavoidable that small isolated bubbles of air will be occluded in the pore sequences thus lowering the water content a small amount below complete saturation and reducing the 'saturated' hydraulic conductivity. However, from a hydraulic viewpoint the soil in this state still behaves as a saturated material, e.g. for homogeneous porous materials h(z) profiles in this zone will be linear and fluxes will be uniform. In addition, since the small quantity of air occluded is not in continuity with the main body of pore air being compressed by the advancing wet front, its presence does not invalidate the theoretical principles detailed in the last section.

Profile depths of 200 cm and 1,000 cm have been analysed for both porous materials. Because the initial condition for the analyses considered in this study was that of uniform θ_i it became unnecessary to solve the finite difference equations for the entire profile depth. Much computational effort was saved by using a reduced profile for the numerical analysis whilst including for the Boyle's Law calculation the entire pore air volume of the 200 cm and 1,000 cm profiles. Under these conditions the lower boundary condition became, in effect, one of constant pressure, h_i, at a point removed from the influence of possible wetting A satisfactory reduced depth was 100 cm for this study.

The point of departure of the present analysis from the normal infiltration analysis is the inclusion of the time-dependent surface boundary condition to model the air pressure increases. The effect of this boundary condition on h(z) profiles for #17 sand for L = 1,000 cm may be noted from Fig. 6. As infiltration proceeds h at the surface decreases, resulting finally in h(z) profiles which exhibit a moderate increase in h (i.e. less negative) over most of the profile above the wet front region. For purposes of comparison the h(z) profile for normal infiltration for t = 5 min is also included in Fig.6. As expected this relationship exhibits a uniform decrease of h down the profile in the developing saturated zone.

In the previous section of this paper it was noted that for the maintenance of continued downward water movement in the profile, H must decrease with depth, resulting in the drainage of parts of the soil profile. This effect can be clearly demonstrated by superimposing on the $h(\theta)$ characteristic the paired values of h and θ existing at different depths in the profile at a given time. #17 sand with L = 200 cm and t = 8 min (t_d) has been chosen and the results are plotted in Fig.7. At t = 8 min the surface pressure (marked as z=0 in Fig.7) is almost equal to the air entry value (-34.0 cm); at -2 cm h has increased to -32 cm although θ is still at the saturated value. Below -2 cm the $h(\theta)$ profile takes the form shown in Fig.7 and connects with the boundary wetting curve at approximately -10 cm. Accordingly, all points above -10 cm are either draining or remaining at the θ_{sat} value. Although the $h(\theta)$ profile in Fig.7 for the draining zone exhibits considerable pressure departures from the boundary wetting curve the volume of water drained after the reversal is not large due to the 'flat' shape of the primary draining scanning curves at the points of departure from the boundary wetting curve. This is illustrated with the data for z = -4 cm. Fig.7 shows the reversal occurring at -21.0 cm and indicates the path followed at times of 0.5, 1, 3 and 8 min. Although the pressure decreases from -21.0 cm to -30.2 cm, θ only changes from 0.243 $cm^3\ cm^{-3}$ to 0.233 $cm^3\ cm^{-3}$. This small θ decrease results in a $\theta(z)$ profile which maintains a reasonably stable position at those elevations which have experienced reversal. Although the θ change is small following reversal there is considerable difference between such values and the θ_{sat} value, which would have been the θ condition if the -4 cm point has been permitted to follow the

boundary wetting curve to the water entry value and hence saturation.

Fig.8 gives the $\theta(z)$ profiles for #17 sand for L = 200 cm and L = 1,000 cm at several times. For the 200 cm depth $\theta(z)$ profiles at times of 0.5, 3 and 8 min (t_d) are given. In this case the air pressure increases quite rapidly being equal to 22 cm of water (see Fig.14) at 0.5 min resulting in an early inhibition of $\theta(z)$ development. At 3 min the air pressure has risen to 30 cm and limited additional infiltration occurs. However, in the period from 3 to 8 min the incremental infiltration volume is small. As discussed previously the $\theta(z)$ profile is sensibly stable over most of its depth during the 3-8 min interval. For the 1,000 cm profile the effect is less dramatic although the same $\theta(z)$ shape trends are present. Since the air pressure increase occurs much more slowly, the infiltrating water penetrates much deeper into the profile than with the 200 cm depth. The greater penetration is quite significant, particularly as the t_d value of 10.5 min for the 1,000 cm depth is not greatly in excess of the 8.0 min value of the 200 cm depth. Similar results are presented in Fig.9 for the Rubicon sandy loam. For L = 200 cm, $\theta(z)$ profiles at times of 2, 10 and 38 min (t_d) are given. Near the surface the $\theta(z)$ profile never fully develops but remains stable. For L = 1,000 cm greater $\theta(z)$ profile development occurs in the lower part of the profile although the upper section again approaches a stable condition. For this case t_d = 396 min.

A comparison of the shapes and positions of the wetting fronts is given in Figs.10 and 11 for #17 sand and Rubicon sandy loam respectively. For #17 sand the comparison is made after 4 min of infiltration and for the sandy loam after 30 min of infiltration. Included in both figures is the $\theta(z)$ curve for normal infiltration at the specified times. For #17 sand and L = 200cm the wet front is considerably retarded in its position compared with the normal condition as would be expected. In addition the shape of the front is more diffuse due to the drainage effect. The shape changes are less significant for L = 1,000 cm. For the Rubicon sandy loam a significant feature of Fig.11 is the manner in which only the surface values attain saturation for L = 200 cm and L = 1,000 cm. This condition is maintained until t_d is reached as Fig.9 indicates. This is in contrast to the normal infiltration case where a saturated zone develops from the surface as infiltration continues. Fig.11 highlights again the considerable shape difference in the $\theta(z)$ profiles.

Figs.12 and 13 compare the cumulative infiltration relationships for #17 sand and the sandy loam. For both porous materials the limitation which the air compression has on cumulative infiltration when L = 200 cm is most marked. As the $\theta(z)$ profiles revealed, the cumulative infiltration when L = 1,000 cm is greatly increased compared with the 200 cm case. However the volume infiltrated, particularly in the case of the Rubicon sandy loam, is much less than the normal infiltration condition.

REFERENCES

1. Philip, J.R. (1969). Theory of infiltration. Advances in Hydrosci., 5:216-296.
2. Phuc, L.V. and Morel-Seytoux, H.J. (1972). Effect of soil air movement and compressibility on infiltration rates. Soil Sci. Soc. Amer. Proc., 36:237-241.
3. Powers, W.L. (1934). Soil water movement as affected by confined air. J. Agr. Research, 49:1125-1133.
4. Free, G.R. and Palmer, V.J. (1940). Inter-relationship of infiltration, air movement and pore size in graded silica sand. Soil Sci. Soc. Amer. Proc., 5:390-398.
5. Wilson, L.G. and Luthin, J.N (1963). Effect of air flow ahead of the wetting front on infiltration. Soil Sci., 96 136-143.
6. Youngs, E.G. and Peck, A.J. (1964). Moisture profile development and air compression during water uptake by bounded porous bodies: 1. Theoretical introduction. Soil Sci., 98:290-294.
7. Peck, A.J. (1965). Moisture profile development and air compression during water uptake by bounded porous bodies: 2. Horizontal columns. Soil Sci , 99:327-334.
8. Peck, A.J. (1965). Moisture profile development and air compression during water uptake by bounded porous bodies: 3. Vertical columns. Soil Sci., 100:44-51.
9. Whisler, F.D. and Klute, A. (1967). Rainfall infiltration into a vertical soil column Trans. Amer. Soc. Agric. Eng., 10 391-395.
10. Whisler, F.D. and Watson, K.K (1968). One-dimensional gravity drainage of uniform columns of porous materials. J. of Hydrology, 6:277-296.
11. Whisler, F.D. and Watson, K.K. (1969). Infiltration into draining porous media. J. Irrig. and Drainage Div., ASCE, 95 (IR4):481-491.
12. Topp, G.C. (1969). Soil-water hysteresis measured in a sandy loam and compared with the hysteretic domain models. Soil Sci. Soc. Amer. Proc., 33:645-651

ACKNOWLEDGEMENTS

The financial assistance of the Australian Research Grants Committee is acknowledged with thanks.

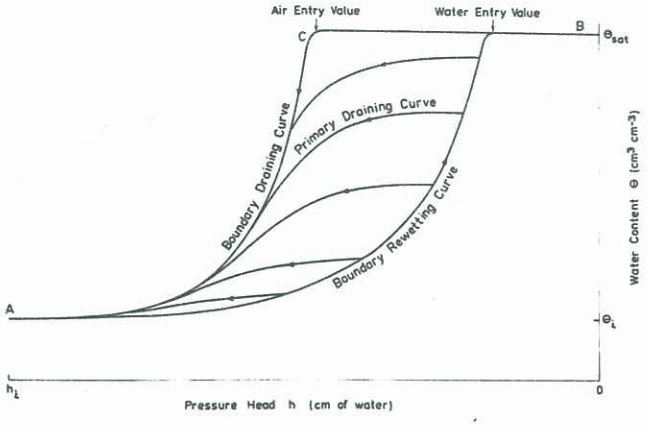

Fig. 1 Generalized h(θ) relationships.

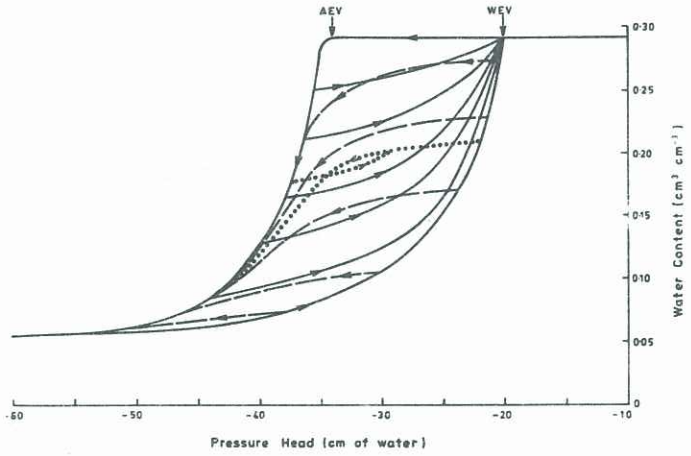

Fig. 2 h(θ) relationships for #17 sand.

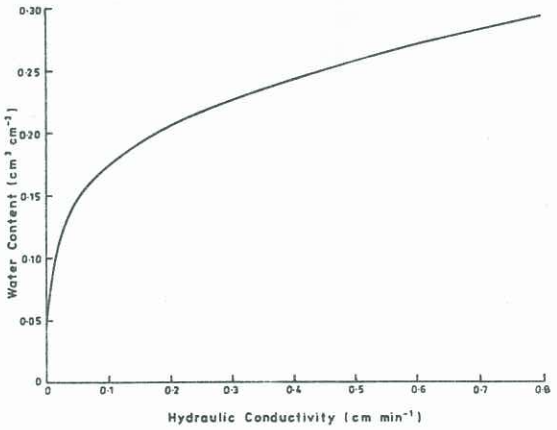

Fig. 3 K(θ) relationship for #17 sand.

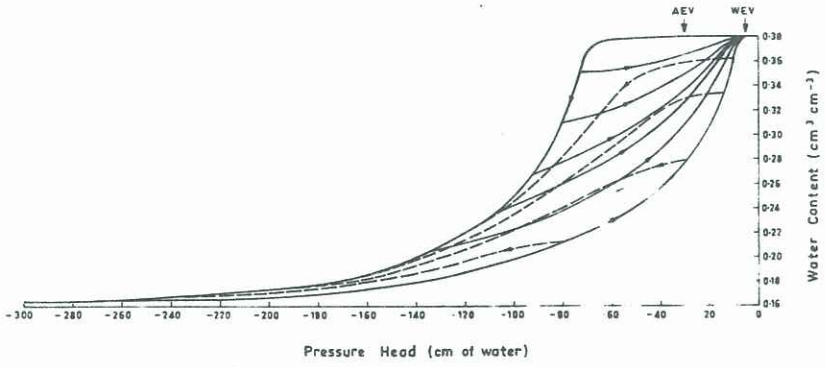

Fig. 4 h(θ) relationships for Rubicon sandy loam.

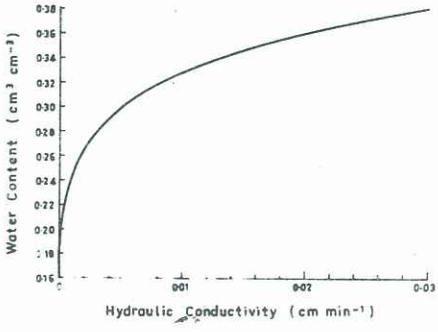

Fig. 5 K(θ) relationship for Rubicon sandy loam.

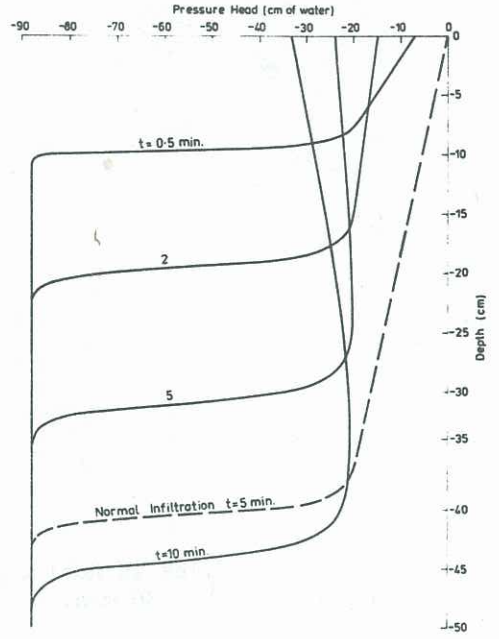

Fig. 6 Pressure head profiles in #17 sand for L = 1000 cm.

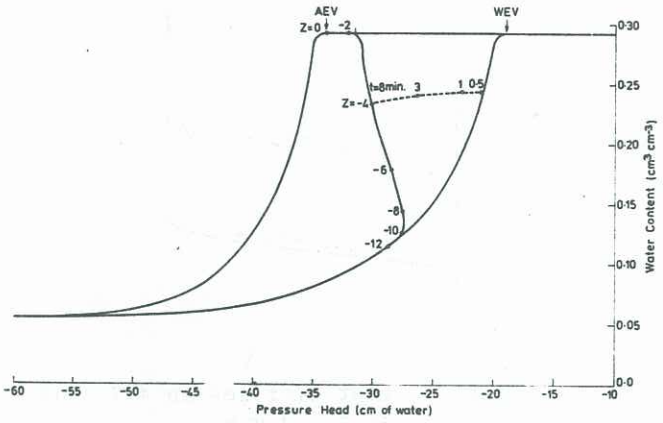

Fig. 7 h(θ) relationship for #17 sand for L = 1000 cm and t = 8 min.

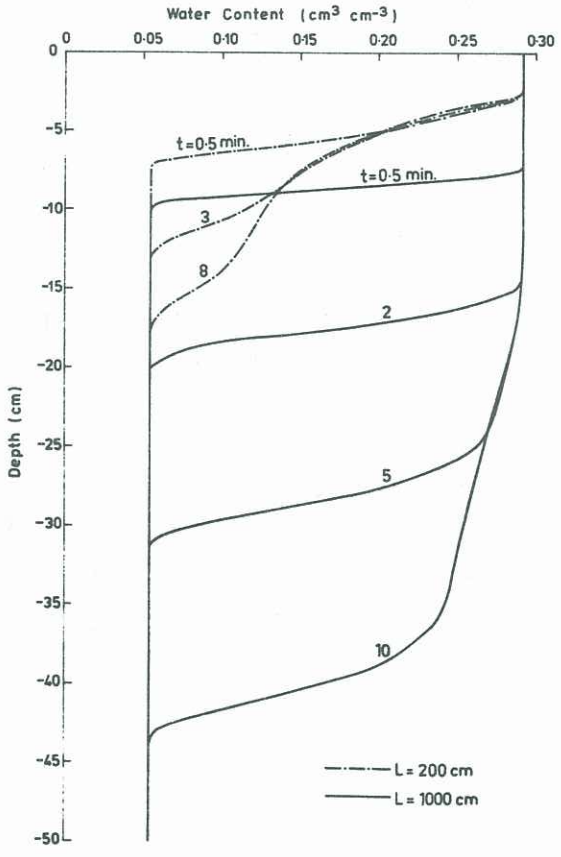

Fig. 8 Water content profiles in #17 sand for L = 200 cm and L = 1000 cm.

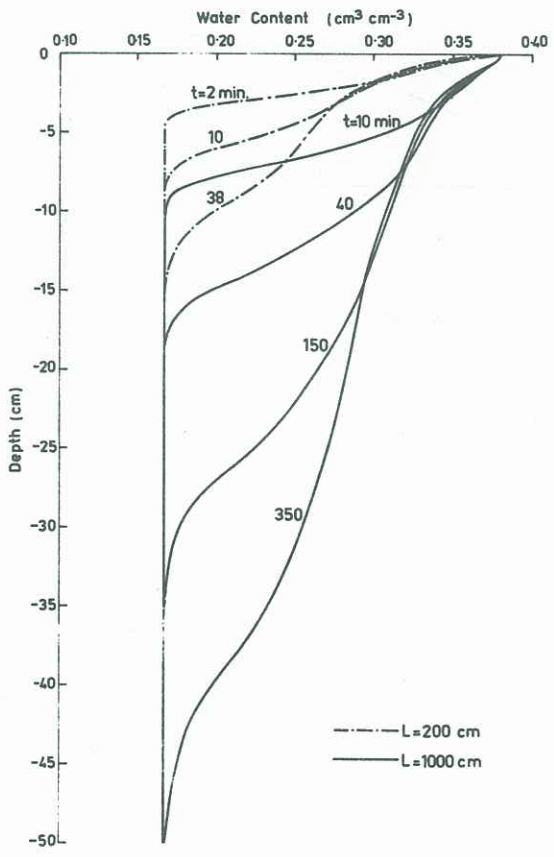

Fig. 9 Water content profiles in Rubicon sandy loam for L = 200 cm and L = 1000 cm.

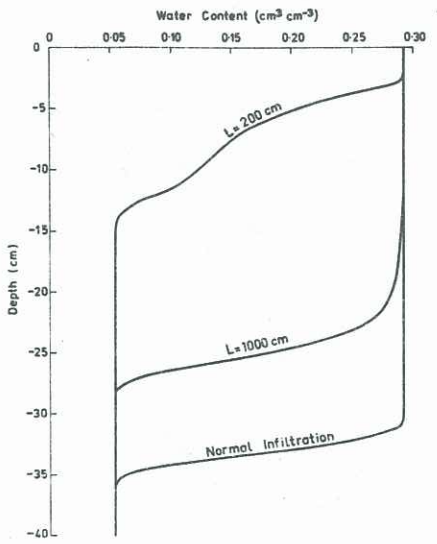

Fig.10 Water content profiles in #17 sand at t = 4 min.

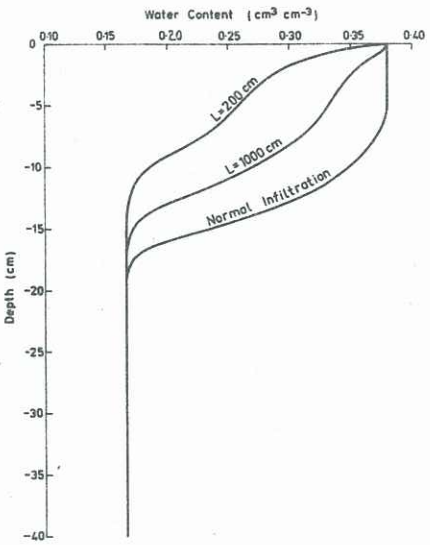

Fig.11 Water content profiles in Rubicon sandy loam at t = 30 min.

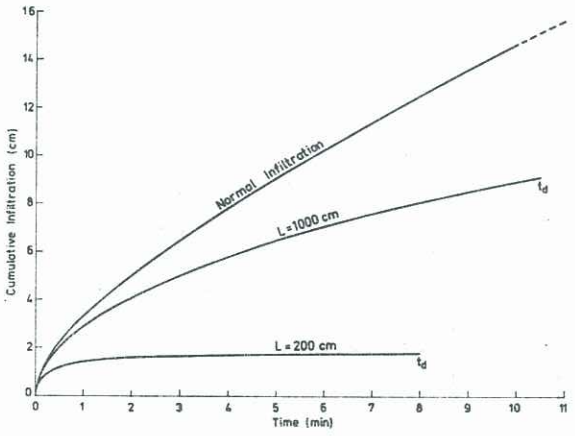

Fig.12 Relationships between time and cumulative infiltration for #17 sand.

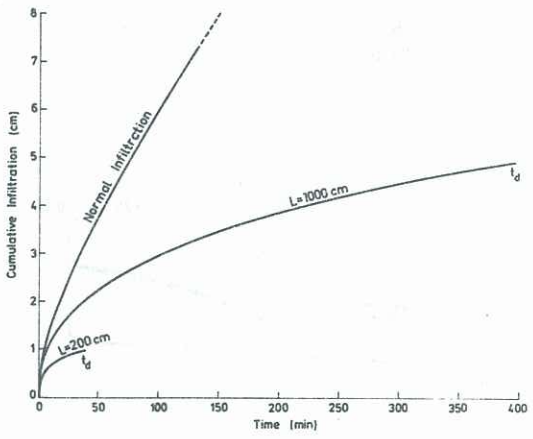

Fig.13 Relationships between time and cumulative infiltration for Rubicon sandy loam.

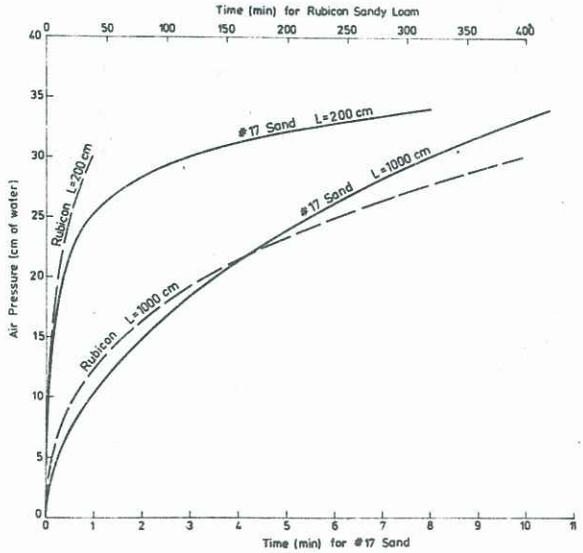

Fig.14 Relationships between time and air pressure for #17 sand & Rubicon sandy loam.